# Metal-Centered Deltahedral Zintl Ions: Synthesis of [Ni@Sn₉]⁴⁻ by Direct Extraction from Intermetallic Precursors and of the Vertex-Fused Dimer [{Ni@Sn₈(μ-Ge)₁/₂}₂]⁴⁻

Miriam M. Gillett-Kunnath, Joseph I. Paik, Sara M. Jensen, Jacob D. Taylor, and Slavi C. Sevov*

Department of Chemistry and Biochemistry, University of Notre Dame, Notre Dame, Indiana 46556, United States

S *Supporting Information*

ABSTRACT: Ni-centered deltahedral Sn_9 clusters with a charge of 4−, i.e., $[Ni@Sn_9]^{4-}$, were extracted in ethylenediamine in high yield directly from intermetallic precursors with the nominal composition "$K_4Sn_9Ni_3$". The new endohedral clusters were crystallized and structurally characterized in K[K-(18-crown-6)]₃[Ni@Sn₉]·3benzene (**1a**, triclinic, $P\bar{1}$, $a = 10.2754(5)$ Å, $b = 19.5442(9)$ Å, and $c = 20.5576(13)$ Å, $\alpha = 73.927(3)°$, $\beta = 79.838(4)°$, and $\gamma = 84.389(3)°$, $V = 3899.6(4)$ Å³, $Z = 2$) and K[K(2,2,2-crypt)]₃[Ni@Sn₉] (**1b**, triclinic, $P\bar{1}$, $a = 15.8028(8)$ Å, $b = 16.21350(9)$ Å, and $c = 20.1760(12)$ Å, $\alpha = 98.71040(10)°$, $\beta = 104.4690(10)°$, and $\gamma = 118.3890(10)°$, $V = 4181.5(4)$ Å³, $Z = 2$). The alternative method of a post-synthetic insertion of a Ni atom in empty Sn_9 clusters by a reaction with $Ni(cod)_2$ predominantly produces the more-oxidized clusters with a charge of 3−, i.e., the recently reported $[Ni@Sn_9]^{3-}$. Nonetheless, using substoichiometric amounts of 18-crown-6 as a cation sequestering agent, we also have been able to isolate the 4− clusters as a minor phase from such reactions. They were structurally characterized in K[K(en)][K(18-crown-6)]₂[Ni@Sn₉]·0.5en (**2**, monoclinic, $P2_1/n$, $a = 10.4153(5)$ Å, $b = 25.6788(11)$ Å, and $c = 20.6630(9)$ Å, $\beta = 102.530(2)°$, $V = 5394.7(4)$ Å³, $Z = 2$). The ability of the Ni-centered clusters to exist with both 3− and 4− charges parallels the same ability of the empty clusters and is very promising for similarly rich chemistry involving electron transfer and flexible "oxidation states". We also report the synthesis and characterization of the endohedral heteroatomic dimer $[\{Ni@Sn_8(\mu\text{-}Ge)_{1/2}\}_2]^{4-}$ composed of two $[Ni@(Sn_8Ge)]$-clusters fused at the Ge-vertex. The dimer was synthesized by reacting an ethylenediamine solution of a ternary precursor with the nominal composition "$K_4Ge_{4.5}Sn_{4.5}$", which is known to produce heteroatomic $Ge_{9-x}Sn_x$ clusters, with $Ni(cod)_2$. It is isostructural with the reported $[\{Ni@Sn_8(\mu\text{-}Sn)_{1/2}\}_2]^{4-}$ and is structurally characterized in [K-(2,2,2-crypt)]₄[{Ni@Sn₈(μ-Ge)₁/₂}₂]·2en (**3**, monoclinic, $C2/c$, $a = 30.636(2)$ Å, $b = 16.5548(12)$ Å, and $c = 28.872(2)$ Å, $\beta = 121.2140(10)°$, $V = 12523.5(15)$ Å³, $Z = 4$).
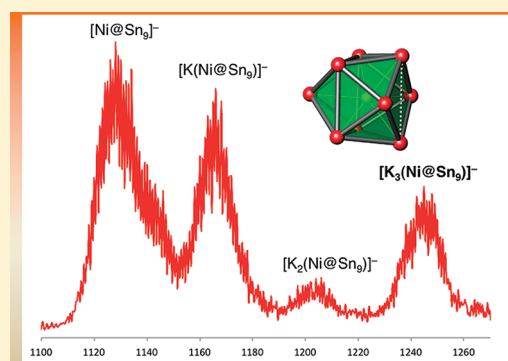
■ INTRODUCTION

Over the past 10−15 years, the chemistry of deltahedral Zintl ions has rapidly soared from virtually nonexistent to a level where it regularly produces exciting results.[1] Many of these results involve reactions of the insertion of transition-metal atoms in the clusters after their extraction in solution. For example, $[Ni@Ge_9]^{3-}$ and $[Ni@Sn_9]^{3-}$ are made by reactions of ethylenediamine solutions of the intermetallic precursors K_4E_9 (E = Ge, Sn) with $Ni(cod)_2$.[2] Similarly, $[Cu@Sn_9]^{3-}$ and $[Cu@Pb_9]^{3-}$ are made by reactions of the corresponding precursors with MesCu (mes = mesityl) in dimethylformamide (DMF).[3] More interestingly, some of these insertion reactions lead to increased nuclearity of the clusters or to new nondeltahedral shapes. Examples are the single-cage 10-atom bicapped square antiprismatic $[Ni@Pb_{10}]^{2-}$,[4,5] the icosahedral $[M@Pb_{12}]^{2-}$ (M = Mn, Ni, Pd, Pt) and $[Ir@Sn_{12}]^{3-}$,[5] the unique pentagonal prismatic $[Co@Ge_{10}]^{3-}$ and $[Fe@Ge_{10}]^{3-}$,[6] and the more-complex $[Ni_2@Sn_{17}]^{4-}$, $[Ni_3@Ge_{18}]^{4-}$, and $[Pt_2@Sn_{17}]^{4-}$, all made of two fused cages.[2a,7,8] Lastly, the 18-atom deltahedral clusters $[Pd_2@Ge_{18}]^{4-}$ and $[Pd_2@Sn_{18}]^{4-}$

represent the largest single-cage deltahedral clusters which, in this case, are stabilized by pairs of central Pd atoms.[9] In addition to these ligand-free species, there are several known endohedral clusters capped by ligated heteroatoms. Examples are $[Ni@Ge_9-Ni(PPh_3)]^{2-}$, $[Ni@E_9-Ni(CO)]^{3-}$, $[Ni@Ge_9-Ni(en)]$, $[Ni@Ge_9-Ni(CCPh)]^{3-}$, $[Ni@Ge_9-Pd(PPh_3)]^{3-}$, $[Pt@Sn_9-Pt(PPh_3)]^{2-}$, and $[Pd@Sn_9-Pd(SnCy_3)]^{3-}$, all capped by various metal−ligand fragments.[10−14] Despite the number of examples, however, not much is known about the reactivity and formation of these endohedral Zintl clusters. At the same time, they are attractive for their potential use as building blocks in cluster-assembled nanoparticles, larger aggregates, and metastable bulk compounds.[15,16]

Interestingly enough, all the centered deltahedral clusters are more oxidized, with respect to the corresponding empty nine-atom clusters E_9^{4-} (E = Ge, Sn, Pb). At the same time, most of

the insertion reactions do not involve redox processes. The most likely reason for this oxidation is the well-known catalyzing effect of traces of transition-metal compounds on the reduction of ethylenediamine (or liquid ammonia) by dissolved alkali metals.[17] On the other hand, in order to study the chemistry of the centered nine-atom clusters and compare them with the corresponding empty clusters, they need to have the same starting charge of 4− as for the empty clusters E_9^{4-}. A strong hint for the existence of such clusters came from the recently reported reactions of both empty and Ni-centered clusters with TlCp to form the corresponding Tl-capped species $[E_9Tl]^{3-}$ and $[Ni@E_9Tl]^{3-}$, respectvely.[2] The similarity of the products suggested similar reaction paths and, therefore, similarly charged starting empty and centered clusters. The existence of E_9^{4-} is well-documented,[1] and its reaction with TlCp proceeds via reduction of the latter to Cp^- and addition of a Tl-vertex to the cluster, i.e., $E_9^{4-} + TlCp \rightarrow [E_9Tl]^{3-} + Cp^-$. The corresponding Ni-centered cluster $[Ni@E_9Tl]^{3-}$ most likely forms along the same reaction pathway but starting from a hypothetical $[Ni@E_9]^{4-}$, i.e., $[Ni@E_9]^{4-} + TlCp \rightarrow [Ni@E_9Tl]^{3-} + Cp^-$.[2b] The eventual existence of such $[Ni@E_9]^{4-}$ clusters in addition to the already reported $[Ni@E_9]^{3-}$ clusters would mean that the Ni-centered E_9 clusters can have variable oxidation states exactly as the empty clusters E_9^{4-} and E_9^{3-}.[1,2] With this in mind, we set upon searching for a synthetic route that would yield consistently high yields of $[Ni@E_9]^{4-}$ in order to study their reactivity further. Herein, we report that direct extraction of intermetallic precursors of nominal composition "K_4Sn_9Ni_3" with ethylenediamine results in high yields of $[Ni@Sn_9]^{4-}$. The corresponding Ge-based precursors, however, provide only empty Ge_9 clusters. The new endohedral clusters were structurally characterized in $K[K(18\text{-crown-}6)]_3[Ni@Sn_9]\cdot 3benzene$ (**1a**) and $K[K(2,2,2\text{-crypt})]_3[Ni@Sn_9]$ (**1b**). Meanwhile, the clusters were also crystallized as the minor product from the insertion reaction of Sn_9^{4-} with $Ni(cod)_2$ as $K[K(en)][K(18\text{-crown-}6)]_2[Ni@Sn_9]\cdot 0.5en$ (**2**). This confirms the speculation that they form in such reactions but are then slowly oxidized to $[Ni@Sn_9]^{3-}$ in a reaction catalyzed by the presence of free $Ni(cod)_2$. The same reaction, but carried out with heteroatomic Ge/Sn clusters extracted from a precursor with nominal composition "K_4Ge_{4.5}Sn_{4.5}", resulted in a dimer of Ni-centered vertex-shared species $[\{Ni@Sn_8(\mu\text{-Ge})_{1/2}\}_2]^{4-}$ structurally characterized in $[K(2,2,2\text{-crypt})]_4[\{Ni@Sn_8(\mu\text{-Ge})_{1/2}\}_2]\cdot 2en$ (**3**).

■ RESULTS AND DISCUSSION

Our recently acquired knowledge that heteroatomic clusters $[Ge_{9-x}Sn_x]^{n-}$ can be extracted in ethylenediamine directly from the corresponding ternary precursors $K_xGe_ySn_z$ gave us the idea to try analogous direct extraction from an appropriate Ni-containing $K_xSn_yNi_z$ ternary precursor.[18] Thus, such precursors were prepared by heating mixtures of the three elements at 950 °C for 48 h, and the precursors with a nominal composition "K_4Sn_9Ni_3" readily dissolved in ethylenediamine, forming an intensely colored red solution. An electrospray mass spectrum (in the negative-ion mode) of this solution provided the first indication that a Ni-centered cluster with a 4− charge is present. The spectrum showed a peak at $m/z = 1244$, which corresponds to $[K_3(Ni@Sn_9)]^-$, in addition to peaks for $[Ni@Sn_9]^-$ ($m/z = 1127$), $[K(Ni@Sn_9)]^-$ (1166), and $[K_2(Ni@Sn_9)]^-$ (1205). Aliquots of the same solution were then layered with benzene or toluene solutions of 18-crown-6 and 2,2,2-crypt and crystals were

recovered after several days: red rods of $K[K(18\text{-crown-}6)]_3$-$[Ni@Sn_9]\cdot 3benzene$ (**1a**) and red blocks of $K[K(2,2,2\text{-crypt})]_3$-$[Ni@Sn_9]$ (**1b**). The latter compound is isostructural with the corresponding compound with empty Sn_9 clusters, $K[K(2,2,2\text{-crypt})]_3[Sn_9]$.[19]

The easy dissolution of the K−Sn−Ni precursor in ethylenediamine with the direct formation of Ni-centered clusters raised the question about the phase contents of the precursor, especially in light of the fact that the corresponding K−Ge−Ni precursor produced only empty Ge_9 clusters (confirmed by ES-MS and single-crystal X-ray diffraction (XRD)). Powder XRD studies of the two precursors revealed very poor crystallinity for both but two very different pictures in the phase contents. Thus, the Ge-based precursor is very inhomogeneous and exhibits the K−Ge binary phase(s) $K_{12}Ge_{17}$ or/and K_4Ge_9 (it is difficult to tell which, because of poor crystallinity), elemental nickel, and $GeNi_2$ ($InNi_2$ type).[20] The Sn-based precursor, on the other hand, is very homogeneous and does not show any recognizable phase, in addition to small amounts of unreacted elemental tin. Importantly, there are no traces of elemental nickel or any other known phase that contains nickel, despite the numerous known binary Ni−Sn phases.[21] Clearly, the nickel has been consumed in a phase that most likely also contains K and Sn. It is also possible that the Ni-centered Sn clusters are already formed in such a phase, perhaps $K_4[Ni@Sn_9]$, analogous to K_4Sn_9, which, when treated with ethylenediamine, releases them into the solution. Unfortunately, we have not been able to isolate good-quality single crystals for XRD studies so far. Perhaps different heat treatments with different temperature profiles, including, for example, annealing, may produce better crystals in the future.

In parallel with the direct extraction studies, we continued our attempts to crystallize the same Ni-centered anions from reactions of E_9^{4-} with $Ni(cod)_2$, although the electrospray mass spectra showed only the 3− species.[2b] The objective of our approach was (a) to reduce the reaction times before layering for crystallization, in order to decrease the possibility for post-synthetic oxidation of eventual $[Ni@E_9]^{4-}$, and (b) to use smaller sequestering agents (18-crown-6 in this case) in smaller amounts in order to allow for the packing of four, instead of three, cations with one anion. Thus, solutions layered with toluene containing only 2 equiv of 18-crown-6 produced a few red-block crystals of $K[K(en)][K(18\text{-crown-}6)]_2[Ni@Sn_9]\cdot 0.5en$ (**2**) after several weeks. The compound is isostructural with the corresponding empty-cluster compounds $A[A(en)][A(18\text{-crown-}6)]_2[Sn_9]\cdot 0.5en$ for A = K, Rb.[22] It is important to note that this approach for the synthesis of $[Ni@Sn_9]^{4-}$ does not provide very reproducible results and high yields.

Structurally, the new Ni-centered clusters (Figure 1) resemble the corresponding empty clusters and can be described as distorted tricapped trigonal prisms (*ttp*), where one of the three trigonal prismatic edges (heights) parallel to the 3-fold axis is elongated (edge 1−4). This elongation leads to flattening of the otherwise butterfly-like shape made of the two triangles adjacent to that elongated edge, i.e., triangles 1−4−7 and 1−4−8 (compare with the "bent" pairs of triangles 3−6−7/3−6−9 and 2−5−8/2−5−9). At some point of the elongation, the distances 1−4 and 7−8 become comparable and, therefore, the almost-planar rhombus 1−7−4−8 becomes a square. At such specific distortion, the overall cluster can be viewed as a mono-capped square antiprism (*msa*) with square bases 1−7−4−8 (uncapped) and 2−3−6−5 (capped by 9). The real picture is often more complicated than this, with not just one but two or

even all three prismatic heights being somewhat elongated, and this makes it difficult to assign a specific shape. In addition, the shape is affected by the charge of the cluster, which defines the number of available valence electrons. Thus, clusters with a charge of 4−, such as Sn_9^{4-} and $[Ni@Sn_9]^{4-}$ have 40 such electrons available (the Ni atom does not contribute electrons; it only participates in cluster orbital overlap with its 4s and 4p orbitals) and, according to the Wade—Mingos electron counting rules for deltahedral clusters, are classified as *nido*-deltahedra.[1] As such, ideally they should be *msa* structures. The clusters with a charge of 3− as Sn_9^{3-} and $[Ni@Sn_9]^{3-}$, on the other hand, have an odd number of valence electrons, 39, and are intermediate between *nido*- and *closo*-deltahedra with 40 and 38 electrons, respectively. Therefore, their shape is expected to be between that of a *closo ttp* and the *nido msa*.

A system for the classification of the shapes of empty 9-atom clusters as close to *ttp* or *msa* was developed by Corbett and used
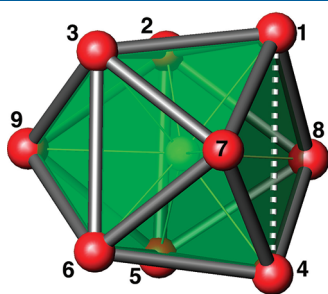

Figure 1. General view of $[Ni@Sn_9]^{4-}$ in compounds **1a**, **1b**, and **2** with the atoms numbered. The cluster can be viewed either as a tricapped trigonal prism (*ttp*) with triangular bases of atoms 1−2−3 and 4−5−6 (atoms 7, 8, and 9 are capping) or as a monocapped square antiprism (*msa*) with square bases of atoms 1−7−4−8 and 2−3−6−5, where the latter is capped by atom 9.

various edge ratios.[23a] It was later expanded by Fässler to involve some dihedral angles.[22b,23b] These parameters for the three compounds reported here are listed in Table 1, together with the parameters for similar compounds with empty clusters as well as the recently reported Ni-centered clusters with a charge of 3−. Beginning with the latter, it has been already discussed that the Ni-insertion leads to elongation of the Sn—Sn distances by as much as 0.3 Å and overall elongation of the cluster along the pseudo-3-fold axis that results in almost a spherical shape.[2b]

Comparison of $[Ni@Sn_9]^{4-}$ and Sn_9^{4-} in the isostructural **2** and $K[K(en)][K(18C6)]_2[Sn_9]\cdot^1/_2en$, respectively, show that all Sn—Sn distances in the centered cluster are slightly longer. However, the overall shapes of the clusters are almost identical, according to the parameters listed in Table 1. In other words, the insertion of the Ni atom in Sn_9^{4-} only expands the cluster but does not change its geometry. This is contrary to the insertion of a Ni atom in Sn_9^{3-} clusters, where the shape of the cluster changes from being somewhat compressed along the pseudo-3-fold axis to being an almost perfectly spherical shape when centered. Both $[Ni@Sn_9]^{4-}$ and Sn_9^{4-} are very close to C_{4v} symmetry (Table 1) and are practically identical with the empty Sn_9^{4-} clusters in $Rb_2[Rb(18C6)]_2[Sn_9]\cdot^1/_2en$,[22b] $K[K(2,2crypt)]_3$-$[Sn_9]$,[19] $[Na(2,2,2crypt)]_4[Sn_9]$,[23a] and $Cs_7[K(2,2,2crypt)]$-$[Sn_9]_2\cdot3en$.[23b] This symmetry for $[Ni@Sn_9]^{4-}$ and the observed broad range of Ni—Sn distances, 2.487(3)−2.784(2) Å, when compared to $[Ni@Sn_9]^{3-}$ (2.56−2.74 Å), indicate significant deviation from a spherical shape. There are actually three very different sets of Ni—Sn distances in $[Ni@Sn_9]^{4-}$: the distance to the capping atom 9 is the longest, 2.784(2) Å; the distances to the capped square are the shortest, 2.487(3)−2.494(3) Å (average = 2.491 Å); and those to the open square face are intermediate, 2.584(3)−2.618(2) Å (average = 2.600 Å). A comparison with the distances at the centroid of the empty Sn_9^{4-} cluster in $K[K(en)]$-$[K(18C6)]_2[Sn_9]\cdot^1/_2en$ (2.768 Å to the capping atom, 2.435 Å to the capped square, 2.613 Å to the open square) indicates that the

Table 1. Geometric Parameters for Some Empty and Ni-Centered Sn₉ Clusters[a]

compound	ref	cbe	Viewed as a Tricapped Trigonal Prism (*ttp*)					Viewed as a Monocapped Square Antiprism (*msa*)				
			h_1	h_2	h_3	γ	h/e	α_1	α_2	α_3	d_2/d_1	
$[K(2,2,2crypt)]_6[Ni@Sn_9]_2\cdot3en\cdot tol$	2b	21	1.21	1.17	1.02	11	1.13	19	20	34	1.18	$\sim C_{2v}$
$[K(2,2,2crypt)]_6[Sn_9]_2\cdot1.5en\cdot0.5tol$	26	21	1.10	1.02	1.00	6	1.08	13	19	23	1.34	$\sim D_{3h}$
$[K(2,2,2crypt)]_3[Sn_9]\cdot1.5en$	27	21	1.04	1.04	1.02	1	1.08	17	18	18	1.45	D_{3h}
$K[K(18C6)]_3[Ni@Sn_9]\cdot3benz$ (**1a**)		22	1.26	1.08	1.05	14	1.16	7	27	31	1.09	$\sim C_{4v}$
$K[K(2,2,2crypt)]_3[Ni@Sn_9]$ (**1b**)		22	1.31	1.12	1.07	16	1.19	6	28	33	1.04	$\sim C_{4v}$
$K[K(2,2,2crypt)]_3[Sn_9]$	19	22	1.29	1.03	1.00	22	1.19	2	28	29	1.02	C_{4v}
$K[K(en)][K(18C6)]_2[Ni@Sn_9]\cdot^1/_2en$ (**2**)		22	1.31	1.02	1.01	21	1.15	0	30	31	1.01	C_{4v}
$K[K(en)][K(18C6)]_2[Sn_9]\cdot^1/_2en$	22a	22	1.29	1.00	1.00	21	1.15	1	28	29	1.02	C_{4v}
$Rb_2[Rb(18C6)]_2[Sn_9]\cdot^1/_2en$	22b	22	1.33	1.02	0.99	19	1.16	3	29	33	1.04	C_{4v}
$K[K(18C6)]_3[Sn_9]\cdot en$	28	22	1.17	1.06	1.05	8	1.15	13	22	24	1.21	$\sim C_{2v}$
$[K(18C6)]_4[Sn_9]$	28	22	1.11	1.08	1.04	4	1.14	15	17	22	1.32	$\sim D_{3h}$
$Na_4[Sn_9]\cdot7en$	29	22	1.19	1.16	0.99	13	1.19	13	16	34	1.19	$\sim C_{2v}$
$[Na(2,2,2crypt)]_4[Sn_9]$	23a	22	1.32	1.04	1.01	22	1.19	3	29	30	1.01	C_{4v}
$Cs_7[K(2,2,2crypt)][Sn_9]_2\cdot3en$	23b	22	1.29	1.00	1.00	22	1.17	1	28	29	1.01	C_{4v}
$[K(2,2,2-crypt)]_4[Ni_2GeSn_{16}]\cdot2en$ (**3**)		22	1.33	1.33	0.93	26	1.23	16	16	39	1.01/1.01	C_{2v}
		22	1.32	1.32	0.97	23	1.24	16	16	40	1.01/1.01	C_{2v}

[a] Legend: *cbe*, cluster-bonding electrons; h_{1-3}, trigonal prism heights (edges 1−4, 2−5, 3−6 in Figure 1), scaled to 3.194 Å (the shortest height in ref 26); γ, the dihedral angle between the triangular bases (triangles 1−2−3 and 4−5−6 in Figure 1); h/e, the ratio of the averaged trigonal prismatic heights (1−4, 2−5, 3−6) and basal edges (1−2, 2−3, etc.); α_{1-3}, dihedral angles at the three prismatic heights h_{1-3} (triangles 1−4−7/1−4−8, 3−6−7/3−6−9, 2−5−8/2−5−9); and d_2/d_1, the ratio of the diagonals in the open "square" 1−7−4−8 (i.e., 7−8/1−4).
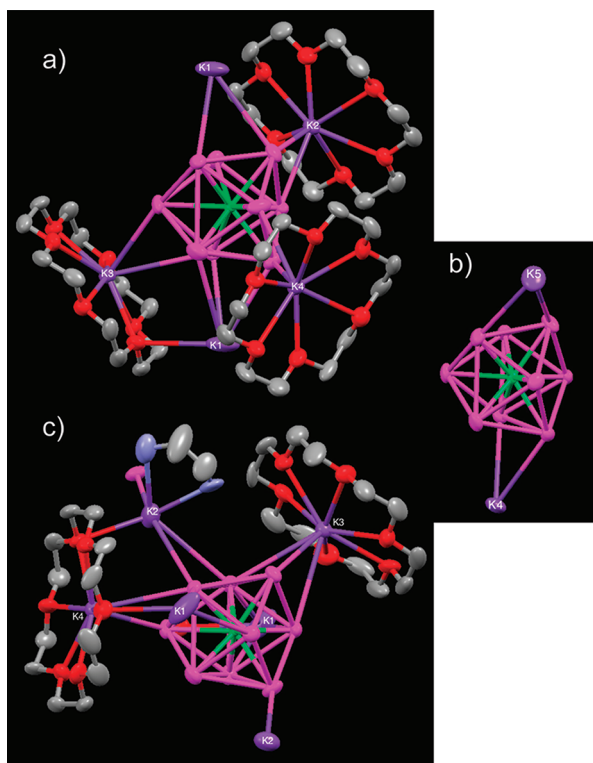
Figure 2. Coordination of the clusters in (a) **1a**, (b) **1b**, and (c) **2** with exposed K cations.

Figure 3. Dimer of vertex-fused nine-atom clusters, $[\{Ni@Sn_8(\mu\text{-}Ge)_{1/2}\}_2]^{4-}$. The two halves are almost identical and can be described as tricapped trigonal prisms (*ttp*) with two elongated prism heights (broken line). The elongations result in two almost-square open faces for each cluster.

Ni atom in the centered cluster is slightly shifted from the center toward the open square face. The reason for this is most likely the otherwise unreasonably short Ni–Sn distances to the atoms of the capped square while keeping the C_{4v} symmetry. For comparison, the Ni–Sn distances in the intermetallic phase Ni_3Sn_4 range from 2.535 Å to 2.772 Å,[24] and the sum of the covalent radii of the two elements is 2.629 Å.[25]

The three sets of Ni–Sn distances (to the capping atom, to the capped square, and to the open square) for compounds **1a** and **1b** are, respectively, 2.7383(9), 2.5215(9)−2.5362(9), and 2.5724-(9)−2.6523(9) Å for **1a** and 2.7318(8), 2.5797(8)−2.5846(8), and 2.6223(8)−2.6402(8) Å for **1b**. It is not clear why, but these distances are noticeably longer than the distances in **2**. They are also much closer to each other, resulting in a narrower overall range of distances. The reason for this is most likely the more spherical shapes for these clusters, which deviate much more from an *msa* (C_{4v}; see Table 1) toward a distorted *ttp* (C_{2v}). This brings them somewhat closer to the 3− cluster, $[Ni@Sn_9]^{3-}$, which, as already mentioned, has a very narrow range of Ni–Sn distances and is much more spherical. Among the most likely reasons for these subtle differences between the clusters in **1a**, **1b**, and **2** are different packing requirements and different cluster−cation interactions (discussed below).

All three compounds **1a**, **1b**, and **2** exhibit cation−cluster electrostatic interactions (Figure 2), since they all have either naked cations as in **1b** or both naked and seminaked, i.e., only planary sequestered by the 18-crown-6 ring or partially coordinated by ethylenediamine, cations as in **1a** and **2**, respectively. The sequestered cations coordinate to only one cluster while the others are shared by pairs of clusters, and they all cap faces or bridge edges of the clusters. The structures of the empty-cluster analogues of **1b** and **2** have been discussed in detail in the
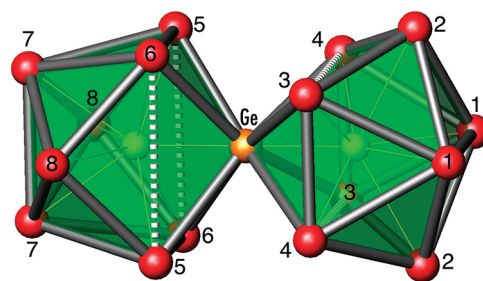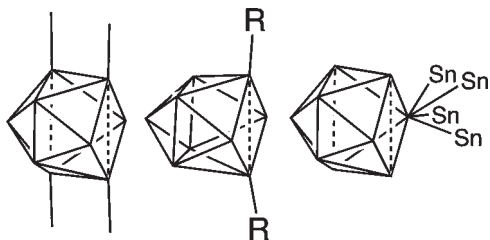
corresponding publications,[19,22a] but some features will be mentioned here again for the purpose of comparison. Thus, the clusters in **1b** interact with two naked K cations (K4 and K5 in Figure 2), and each of them is shared with another identical cluster. The clusters in **2**, on the other hand, exhibit interactions with six K cations of which two (K3 and K4) are sequestered by 18-crown-6 molecules. The remaining four cations (a pair of naked K1 and a pair of ethylenediamine-coordinated K2) are shared with other identical clusters. The cluster−cation interactions in **1a** are very similar to those in **2**, namely each cluster is surrounded by some cations that are sequestered by crown ether molecules (K2, K3, and K4) and others that are shared between clusters (a pair of naked K1). Often structures like these with direct cluster−cation interactions and shared cations are discussed as containing infinite features such as chains or layers made of clusters and cations. Such interpretation suggests bonding interactions between the cations and the clusters that are in addition to and supplement the simple electrostatic attraction between them. The latter is viewed to be the case only when the cations are completely sequestered by 2,2,2-crypt and cannot have direct contacts with the clusters. Consistent with such interpretation would be longer interatomic distances in clusters with cluster−cation direct interactions due to the "additional" nonelectrostatic cluster−cation bonding that can only come for the expense of bonding within the cluster. However, using the three structures at hand, it is very clear that this is not the case at all. The average Sn−Sn distances of the clusters in **1a**, **1b**, and **2** are 3.107, 3.153, and 3.089 Å (including the three prism heights h_{1-3} in Table 1), respectively, and they clearly do not increase with the number of cluster−cation interactions, which are correspondingly 5, 2, and 6. This supports the view that the cluster−cation interactions are just electrostatic, independent of whether the cation is exposed or completely wrapped by the sequestering agent, and extended structures do not exist in such systems.

While working on Ni insertion in preformed Sn_9 and Ge_9 clusters, we also tried the same process for the corresponding heteroatomic clusters $[Ge_{9-x}Sn_x]$ that can be extracted from mixed K−Ge−Sn precursors and can be functionalized.[18] However, the reactions did not result in the expected nine-atom $[Ni@(Sn_{9-x}Ge_x)]^{n-}$ clusters. Instead, they produced complex dimers of Ni-centered fused clusters of $[Ni_2GeSn_{16}]^{4-}$ (see Figure 3), which were structurally characterized in $[K(2,2,2\text{-}crypt)]_4[Ni_2GeSn_{16}]\cdot2en$ (**3**). The compound is isostructural with the tin-only compound $[K(2,2,2\text{-}crypt)]_4[Ni_2Sn_{17}]\cdot2en$

Scheme 1. Schematic Representation of Various Distortions in a Tricapped Trigonal Prism When Bonded by Pairs of Bond to Two Neighboring Clusters (Left), Bonded to Two Exo-substituents (Center), and Bonded to Another Cluster by Sharing a Vertex, as in 3 (Right)

Scheme 2. Removal of the Two 4-Connected Vertices in a *closo*-Octadecahedron (Left) Results in Two Open-Square Faces, as in the Clusters in 3 (Right)

reported by Eichhorn et al., which contains the isostructural $[Ni_2Sn_{17}]^{4-}$.[7] The dimers are made of two Ni-centered 9-atom clusters fused via one vertex, the single Ge atom in $[Ni_2GeSn_{16}]^{4-}$ and a Sn atom in $[Ni_2Sn_{17}]^{4-}$. Thus, they can be written as $[\{Ni@Sn_8(\mu\text{-Ge})_{1/2}\}_2]^{4-}$ and $[\{Ni@Sn_8(\mu\text{-Sn})_{1/2}\}_2]^{4-}$, respectively. The electron count for these species can be easily understood by the rules developed by Mingos for fused metal clusters which state that the number of required valence electrons equals the sum of the electrons for the two clusters minus the number of electrons for the eliminated fragment (upon fusion) obeying the octet rule. Thus, the dimer $[\{Ni@Sn_8(\mu\text{-Ge})_{1/2}\}_2]^{4-}$ is made of two *nido*-$[Ni@(Sn_8Ge)]^{4-}$ clusters and the eliminated fragment is one Ge atom that is formally Ge^{4-} in order to obey the octet rule, i.e., $2[Ni@(Sn_8Ge)]^{4-} - Ge^{4-} = [\{Ni@Sn_8(\mu\text{-Ge})_{1/2}\}_2]^{4-}$. This means that the number of required valence electrons is 2×40 (for each 9-atom *nido*-cluster) $- 8$ (for Ge^{4-}) $= 72$. This number matches exactly the number of provided valence electrons by the 16 Sn atoms + 1 Ge atom + 4 negative charges. This validation of the electron count suggests that the two fused monomers are *nido*-deltahedra since when applied for *closo*, the charge of the dimer would be zero (2×38 for *closo* $- 8 = 68$, which would be the number of valence electrons provided by $[\{Ni@Sn_8(\mu\text{-Ge})_{1/2}\}_2]^{0}$).

The *nido* assignment is also consistent with the overall shape of the monomers (Figure 3), namely, a *ttp* with two very long and one short (normal) prism heights. The bases of the two trigonal prisms are the two pairs of triangles 5−6−7 (left in Figure 3) and 1−3−4 (right in Figure 3). The capping atoms are a pair of atoms 8 and the shared Ge vertex for one of them (left) and a pair of atoms 2 and the same Ge vertex for the other one. The elongated heights are the edges 5−6, 4.2116(8) Å, and 3−4, 4.2348(8) Å, shown as broken lines in Figure 3, while the third height, the edges 7−7 and 1−1, is normal, with distances of 3.099(1) and 2.973(1) Å, respectively. The same elongated heights in the tin-only dimer, 4.252 and 4.268 Å, are somewhat longer while all other Sn−Sn distances are very similar in the two dimers (averages differ by ∼0.008 Å). The difference is most likely due to the longer Sn−Sn distances to the shared capping Sn atom (average of 3.133 Å), compared to the Sn−Ge distances to the capping Ge-atom (average of 3.047 Å). Similar to the tin-only cluster, where the Ni-$(\mu\text{-Sn})$ distances, 2.3822(5) and 2.3865(5) Å, are extremely short, the Ni-$(\mu\text{-Ge})$ distances are also unusually short, 2.224(1) and 2.229(1) Å. For comparison, the sum of the covalent radii of Ni and Ge is 2.449 Å[25] and a short distance of 2.362 Å is observed in $SrNi_3Ge_2$.[30] The remaining Ni−Sn distances are normal and very similar in the two clusters
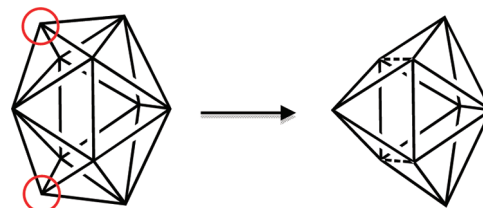
with averages of 2.657 and 2.680 Å in the heteroatomic and homoatomic species, respectively.

The shape of a *ttp* with two long and one short heights (and, thus, two open square-like faces as in 3) is not unusual for *nido* nine-atom clusters. The same shape is observed for the internal Ge_9 clusters in the oligomers $[Ge_9=Ge_9=Ge_9]^{6-}$ and $[Ge_9=Ge_9=Ge_9=Ge_9]^{8-}$. Each of these clusters bond to two neighbors via the four atoms of the long heights, and the intercluster bonds are linear extensions of these heights (Scheme 1, left).[31] In general, the nine-atom deltahedral clusters seem to form exobonds always along elongated heights, i.e., along diagonals (usually the shorter one) of an open square-like face (Scheme 1, middle). Thus, all monosubstituted and disubstituted clusters $[R−E_9]^{3-}$ and $[R−E_9−R]^{2-}$ have the substituents bonded to atoms of one elongated height and the exobonds are linear extensions of that height.[18,32] The common Ge atom in $[Ni_2GeSn_{16}]^{4-}$ can be viewed as a part of one of the two clusters and with external interactions to more than one Sn atoms from the second cluster, four in this case. This would then naturally result in forming not one but two open squarelike faces (Scheme 1, right).[7] Although each cluster of the dimer is a *nido* species, according to the electron count and shape, as already discussed, for purely geometric purposes, it can be also viewed as being derived from the 11-atom *closo*-deltahedron, an octadecahedron (18 triangular faces) by the removal of the two 4-connected vertices, as shown in Scheme 2. This creates two square faces and a shape exactly the same as the clusters in 3.

■ SUMMARY

The endohedral cluster $[Ni@Sn_9]^{4-}$ can be extracted in ethylenediamine from the novel tertiary precursor with nominal composition "$K_4Sn_9Ni_3$". The same clusters can be made in lower yields by the reaction of Sn_9^{4-} with $Ni(cod)_2$; this is a reaction that typically produces $[Ni@Sn_9]^{3-}$ as the major product. The existence of these 4− clusters explains the observed reaction with TlCp to form $[Ni@(Sn_9Tl)]^{3-}$ and Cp^-. It suggests redox reactivity similar to the corresponding empty clusters. Although the analogous Ni-centered Ge clusters $[Ni@Ge_9]^{4-}$ have not been characterized yet, it can be speculated that they also exist, based on the analogous reaction with TlCp and observations of $\{K_3[Ni@Ge_9]\}^-$ in the mass spectra.

■ EXPERIMENTAL SECTION

All manipulations were carried out under nitrogen, using standard Schlenk-line and glovebox techniques. Ethylenediamine (Alfa-Aesar, 99%) was distilled over sodium metal and stored in a gas-tight Schlenk tube under nitrogen in the glovebox. 18-Crown-6 (1,4,7,10,13,16-hexaoxacyclooctadecane, Alfa-Aesar, 99%) was dried by refluxing over sodium metal in diethyl ether and recrystallized from dry *n*-hexanes.

Table 2. Selected Data Collection and Refinement Parameters for Compounds 1−3

	1a	1b	2	3
formula weight	2287.10	2412.78	3724.06	3811.51
space group, Z	$P\bar{1}$, 2	$P\bar{1}$, 2	$P2(1)n$, 2	$C2/c$, 4
a (Å)	10.2754(5)	15.8028(8)	10.4153(5)	30.636(2)
b (Å)	19.5442(9)	16.2350(9)	25.6788(11)	16.5548(12)
c (Å)	20.5576(13)	20.1760(12)	20.6630(9)	28.872(2)
α (deg)	73.927(3)	98.7140(10)		
β (deg)	79.838(4)	104.4690(10)	102.530(2)	121.2140(10)
γ (deg)	84.389(3)	118.3890(10)		
V (Å^3)	3899.6(4)	4181.5(4)	5394.7(4)	12523.5(15)
radiation, λ (Å)		Mo Kα, 0.71073		
ρ_{calcd} (g cm^{-3})	1.948	1.916	2.293	2.022
μ (mm^{-1})	3.241	3.116	4.555	3.846
$R1/wR2$,[a] $I \geq 2\sigma_I$	0.0291, 0.0691	0.0372, 0.0701	0.0253, 0.0447	0.0473, 0.1213
$R1/wR2$,[a] all data	0.0466, 0.0865	0.0585, 0.0782	0.0253, 0.0701	0.0693, 0.1360

[a] $R1 = [\Sigma||F_o| - |F_c||]/\Sigma|F_o|$; $wR2 = \{[\Sigma w[(F_o)^2 - (F_c)^2]^2]/[\Sigma w(F_o^2)^2)]\}^{1/2}$; $w = [\sigma^2(F_o)^2 + (AP)^2 + BP]^{-1}$, where $P = [(F_o)^2 + 2(F_c)^2]/3$ and $A/B =$ 0.0423/0, 0.0209/13.4671, 0/8.3873, 0.0256/214.4017 for **1a**, **1b**, **2**, and **3**, respectively.

Toluene, diethylether, and *n*-hexanes were dried over copper-based catalyst and 4 Å molecular sieve columns (Innovative Technology) and then stored over molecular sieves in the glovebox. Benzene (anhydrous, Acros, 99.0%), DMF (anhydrous DMF, Acros, 99.8%), Ni(cod)$_2$ (cod = cyclooctadiene, Acros, 99%,) were used as received. 2,2,2-Crypt (4,7,13,16,21,24-hexaoxa-1,10-diazabicyclo[8.8.8]hexacosane, Acros, 98%), were used as received, after carefully drying under vacuum.

Synthesis of Precursors. Precursors with nominal compositions K$_4$Sn$_9$, K$_4$Sn$_9$Ni$_3$, and K$_4$Ge$_{4.5}$Sn$_{4.5}$ were synthesized by heating the corresponding mixtures of the elements (K: 99+%, Strem; Ge: 99.999%, Alfa-Aesar; Sn: 99.999%, Alfa-Aesar; Ni, 99.9%, Acros Organics) at 950 °C for two days in sealed niobium containers that were jacketed in evacuated fused-silica ampules.

Synthesis of K[K(18-crown-6)]$_3$[Ni@Sn$_9$]·3benzene (1a) and K[K(2,2,2-crypt)]$_3$[Ni@Sn$_9$] (1b). Two to three milliliters (2−3 mL) of ethylenediamine were added to 0.1 mmol (0.140 g) of a precursor with the nominal composition K$_4$Sn$_9$Ni$_3$ and stirred for 10 − 15 min at room temperature, resulting in a dark red solution. The resulting solution was centrifuged for 15 min and filtered via glass fiber. Aliquots of this solution were used for crystallization by layering with benzene (8 mL) solution of 18-crown-6 (0.293 mmol, 0.077 g) or toluene solution of 2,2,2-crypt (0.293 mmol, 0.11 g). Red blocks of **1a** (yield of ca. 40%) and red rods of **1b** (yield of ca. 35%) crystallized after several days to a week. ES-MS of the reaction mixture prior to crystallization (negative-ion mode; m/z): 1009, (Ni@Sn$_8$)$^-$; 1127, (Ni@Sn$_9$)$^-$; 1166, [K(Ni@Sn$_9$)]$^-$; 1205, [K$_2$(Ni@Sn$_9$)]$^-$; 1255, [K$_3$(Ni@Sn$_9$)]$^-$.

Synthesis of K[K(en)][K(18-crown-6)]$_2$[Ni@Sn$_9$]·en (2). Ethylenediamine (1.5 mL) was added to 0.119 mmol (0.146 g) of a precursor with a nominal composition of K$_4$Sn$_9$ and stirred for 10−15 min at room temperature, resulting in a dark red solution. Ni(cod)$_2$ (0.084 mmol (0.023 g)) was added to the mixture, along with 0.5 mL of ethylenediamine. The addition of Ni(cod)$_2$ formed a green phase within the reaction mixture. The reaction mixture was stirred for 2 h. The resulting light red solution was centrifuged for 15 min and filtered via glass fiber. Aliquots of this solution were used for crystallization by layering with a toluene (8 mL) solution of 18-crown-6 (0.293 mmol, 0.077 g). Red blocks of **2** (yield of ca. 10%) crystallized after several weeks. ES-MS of the reaction mixture prior to crystallization (negative-ion mode; m/z): 1127, (Ni@Sn$_9$)$^-$; 1166, [K(Ni@Sn$_9$)]$^-$.

Synthesis of [K-(2,2,2-crypt)]$_4$[Ni$_2$@GeSn$_{16}$]·2en (3). Three milliliters (3 mL) of ethylenediamine were added to 0.1 mmol (0.102 g) of

a precursor with a nominal composition of K$_4$Ge$_{4.5}$Sn$_{4.5}$ and stirred for 10−15 min at room temperature, resulting in a dark red-brown solution. Ni(cod)$_2$ (0.1 mmol (0.028 g)) was then added and the mixture was stirred for 2 h at room temperature, upon which it turns to a dark brown solution. The resulting brown solution is centrifuged for 15 min and filtered via glass fiber. Aliquots of this solution are used for crystallization by layering with a toluene (8 mL) solution of 2,2,2-crypt (0.293 mmol, 0.11 g). Purple blocks of **3** (yield of ca. 40%) crystallized after several weeks.

Structure Determination. XRD datasets of single crystals of the new compounds were collected at 100 K on Bruker D8 or X8 diffractometers equipped with APEX-II CCD area detectors using graphite-monochromated Mo Kα radiation. The single crystals were selected under Paratone-N oil, mounted on Mitegen micromount loops, and positioned in the cold stream of the diffractometer. The structures were solved by direct methods and refined on F^2 using the SHELXTL V6.21 package.[33] Further details of the data collections and refinements are listed in Table 2.

Mass Spectrometry. Electrospray mass spectra (ES-MS) were recorded on a Micromass Quattro-LC triple quadrupole mass spectrometer (typical conditions: source temperature, 100 °C; desolvation temperature, 125 °C; capillary voltage, 2.5 kV; and cone voltage, 30−65 V) or on a Bruker Microtof-II mass spectrometer (typical conditions: capillary voltage, 3800 V; nebullizer pressure, 0.6 bar; desolvation temperature, 190 °C; capillary exit voltage, 100 V; detector voltage, 1200 V). The samples were introduced by direct infusion with a Harvard syringe pump at 10 μL/min.

■ ASSOCIATED CONTENT

ⓢ Supporting Information. X-ray crystallographic files in CIF format are available free of charge via the Internet at http://pubs.acs.org.

■ AUTHOR INFORMATION

Corresponding Author
*E-mail: ssevov@nd.edu.

■ ACKNOWLEDGMENT

Delaware) for carrying out the powder X-ray diffraction analysis, and Dr. Bill Boggess and CEST for their assistance with the ES-MS experiments.

■ REFERENCES

(1) Reviews:(a) Fässler, T. F. In *Zintl Ions, Principles and Recent Developments*; Fässler, T. F., Ed.; Springer−Verlag: Berlin, Heidelberg: 2011; p 91. (b) Sevov, S. C.; Goicoechea, J. M. *Organometallics* **2006**, *25*, 5678. (c) Fässler, T. F. *Coord. Chem. Rev.* **2001**, *215*, 347. (d) Corbett, J. D. *Angew. Chem., Int. Ed.* **2000**, *39*, 670.

(2) (a) Goicoechea, J. M.; Sevov, S. C. *Angew. Chem., Int. Ed.* **2005**, *44*, 4026. (b) Rios, D.; Gillett-Kunnath, M. M.; Taylor, J. D.; Oliver, A. G.; Sevov, S. C. *Inorg. Chem.* **2011**, *50*, 2373.

(3) Scharfe, S.; Fässler, T. F.; Stegmaier, S.; Hoffmann, S. D.; Ruhland, K. *Chem.—Eur. J.* **2008**, *14*, 4479.

(4) Esenturk, E. N.; Fettinger, J.; Eichhorn, B. W. *Chem. Commun.* **2005**, 247.

(5) (a) Zhou, B.; Krämer, T.; Thompson, A. L.; McGrady, J. E.; Goicoechea, J. M. *Inorg. Chem.* **2011**, *50*, 8028. (b) Esenturk, E. N.; Fettinger, J.; Eichhorn, B. W. *J. Am. Chem. Soc.* **2006**, *128*, 9178. (c) Esenturk, E. N.; Fettinger, J.; Lam, Y.-F.; Eichhorn, B. *Angew. Chem., Int. Ed.* **2004**, *43*, 2132. (d) Wang, J.-Q.; Stegmaier, S.; Wahl, B.; Fässler, T. F. *Chem.—Eur. J.* **2010**, *16*, 1793.

(6) (a) Wang, J. Q.; Stegmaier, S.; Fässler, T. F. *Angew. Chem., Int. Ed.* **2009**, *48*, 1998. (b) Zhou, B.; Denning, M. S.; Kays, D. L.; Goicoechea, J. M. *J. Am. Chem. Soc.* **2009**, *131*, 2802.

(7) Esenturk, E. N.; Fettinger, J.; Eichhorn, B. W. *J. Am. Chem. Soc.* **2006**, *128*, 12.

(8) Kesanli, B.; Halsig, J. E.; Zavalij, P.; Fettinger, J. C.; Lam., Y.-F.; Eichhorn, B. W. *J. Am. Chem. Soc.* **2007**, *129*, 4567.

(9) (a) Goicoechea, J. M.; Sevov, S. C. *J. Am. Chem. Soc.* **2005**, *127*, 7676. (b) Sun, Z.-M.; Xiao, H.; Li, J.; Wang, L.-S. *J. Am. Chem. Soc.* **2007**, *129*, 9560. (c) Kocak, F. S.; Zavalij, P.; Lam, Y. F.; Eichhorn, B. W. *Inorg. Chem.* **2008**, *47*, 3515.

(10) Initially, the anion was reported as Ge-centered, i.e., $[Ge@Ge_9Ni-PPh_3]^{2-}$ (see Gardner, D. R.; Fettinger, J.; Eichhorn, B. *Angew. Chem., Int. Ed. Engl.* **1996**, *35*, 2852). However, this was later corrected to $[Ni@Ge_9Ni-PPh_3]^{2-}$ (see Esenturk, E. N.; Fettinger, J.; Eichhorn, B. *Polyhedron* **2006**, *25*, 521).

(11) Kesanli, B.; Fettinger, J.; Gardner, D. R.; Eichhorn, B. *J. Am. Chem. Soc.* **2002**, *124* (17), 4779.

(12) Goicoechea, J. M.; Sevov, S. C. *J. Am. Chem. Soc.* **2006**, *128*, 4155.

(13) Sun, Z.-M.; Zhao, Y.-F.; Li, F.; Wang, L.-S. *J. Cluster Sci.* **2009**, *20*, 601.

(14) Kocak, F. S.; Zavalij, P.; Eichhorn, B. *Chem.—Eur. J.* **2011**, *17*, 4858.

(15) (a) Fässler, T. F. *Z. Anorg. Allg. Chem.* **1998**, *624*, 569. (b) Guloy, A. M.; Ramlau, R.; Tang, Z.; Schnelle, W.; Baitinger, M.; Grin, Y. *Nature* **2006**, *443*, 320. (c) Guloy, A. M.; Tang, Z.; Ramlau, R.; Böhme, B.; Baitinger, M.; Grin, Y. *Eur. J. Inorg. Chem.* **2009**, *17*, 2455. (d) Chandrasekharan, N.; Sevov, S. C. *J. Electrochem. Soc.* **2010**, *157* (4), C140–C145.(e) Aramatas, G. S.; Kanatzidis, M. G. In *Zintl Ions, Principles and Recent Developments*; Fässler, T. F., Ed.; Springer−Verlag: Berlin, Heidelberg: 2011; p 133.

(16) (a) Zheng, W. J.; Thomas, O. C.; Lippa, T. P.; Xu, S. J.; Bowen, K. H. *J. Chem. Phys.* **2006**, 124. (b) Riley, A. E.; Tolbert, S. H. *Res. Chem. Int.* **2007**, *33*, 111. (c) Sun, D.; Riley, A. E.; Cadby, A. J.; Richman, E. K.; Korlann, S. D.; Tolbert, S. H. *Nature* **2006**, *441*, 1126. (d) Seifert, G. *Nature* **2004**, *3*, 77.

(17) Watt, G. W. *Chem. Rev.* **1950**, *46*, 289.

(18) Gillett-Kunnath, M. M.; Petrov, I.; Sevov, S. C. *Inorg. Chem.* **2010**, *48*, 721.

(19) Burns, R. C.; Corbett, J. D. *J. Am. Chem. Soc.* **1982**, *104*, 2804.

(20) See, for example:(a) Ikeda, T. *J. Phase Equilib.* **1999**, *20*, 626. (b) Nash, A. *Bull. Alloy Phase Diagrams* **1987**, *8*, 255.

(21) See, for example:(a) Liu, H. S.; Wang, J.; Jin, Z. P. *Comput. Coupling Phase Diagrams Thermochem.* **2004**, *28*, 363. (b) Nash, P.; Nash, A. *Bull. Alloy Phase Diagrams* **1985**, *6*, 350.

(22) (a) Hauptmann, R.; Fässler, T. F. *Z. Kristallogr. NCS* **2003**, *218*, 458. (b) Hauptmann, R.; Fässler, T. F. *Z. Anorg. Allg. Chem.* **2002**, *628*, 1500.

(23) (a) Corbett, J. D.; Edwards, P. A. *J. Am. Chem. Soc.* **1977**, *99*, 3313. (b) Hauptmann, R.; Hoffmann, R.; Fässler, T. F. *Z. Anorg. Allg. Chem.* **2001**, *627*, 2220.

(24) Jeitschko, W.; Jaberg, B. *Acta Crystallogr., Sect. B: Struct. Crystallogr. Cryst. Chem.* **1982**, *B38*, 598.

(25) Pauling, L.; Kamb, B. *Proc. Natl. Acad. Sci. (USA)* **1986**, *83*, 3569.

(26) Fässler, T. F.; Hunziker, M. *Z. Anorg. Allg. Chem.* **1996**, *622*, 837.

(27) Critchlow, S. C.; Corbett, J. D. *J. Am. Chem. Soc.* **1983**, *105*, 5715.

(28) Fässler, T. F.; Hoffmann, R. *Angew. Chem.* **1999**, *111*, 526. *Angew. Chem., Int. Ed.* **1999**, *38* (4), 543.

(29) Diehl, L.; Khodadadeh, K.; Kummer, K.; Strähle, J. *Chem. Ber.* **1976**, *109*, 3404.

(30) Hlukhyy, V.; Fässler, T. F. *Z. Anorg. Allg. Chem.* **2008**, *634*, 2316.

(31) (a) Ugrinov, A.; Sevov, S. C. *J. Am. Chem. Soc.* **2002**, *124*, 10990. (b) Yong, L.; Hoffmann, S. D.; Fässler, T. F. *Z. Anorg. Allg. Chem.* **2004**, *631*, 1149. (c) Ugrinov, A.; Sevov, S. C. *Inorg. Chem.* **2003**, *42*, 5789. (d) Yong, L.; Hoffmann, S. D.; Fässler, T. F. *Z. Anorg. Allg. Chem.* **2004**, *630*, 1977.

(32) (a) Ugrinov, A.; Sevov, S. C. *J. Am. Chem. Soc.* **2002**, *124*, 2442. (b) Ugrinov, A.; Sevov, S. C. *J. Am. Chem. Soc.* **2003**, *125*, 14059. Ugrinov, A.; Sevov, S. C. *Chem.—Eur. J.* **2004**, *10*, 3727. (c) Ugrinov, A.; Sevov, S. C. *Chem.—Eur. J.* **2004**, *10*, 3727. (d) Hull, M.; Ugrinov, A.; Petrov, I.; Sevov, S. C. *Inorg. Chem.* **2007**, *46*, 2704. (e) Hull, M.; Sevov, S. C. *Angew. Chem., Int. Ed.* **2007**, *46*, 6695. (f) Hull, M.; Sevov, S. C. *Inorg. Chem.* **2007**, *46*, 10953. (g) Chapman, D. J.; Sevov, S. C. *Inorg. Chem.* **2008**, *47*, 6009. (h) Hull, M.; Sevov, S. C. *J. Am. Chem. Soc.* **2009**, *131*, 9026. (i) Kocak, F. S.; Zavalij, P. Y.; Lam, Y.-F.; Eichhorn, B. W. *Chem. Commun.* **2009**, 4197.

(33) Sheldrick, G. M. *SHELXTL*, Version 6.21; Bruker−Nonium AXS: Madison, WI, 2001.